



Title	As-cast Austenite Grain Structure in Al Added 0.2 wt% Carbon Steel
Author(s)	Kencana, Surya; Ohno, Munekazu; Matsuura, Kiyotaka; Isobe, Kohichi
Citation	ISIJ International, 50(2), 231-238 https://doi.org/10.2355/isijinternational.50.231
Issue Date	2010-02-15
Doc URL	http://hdl.handle.net/2115/75409
Rights	著作権は日本鉄鋼協会にある
Type	article
File Information	ISIJ Int. 50(2)_ 231-238 (2010).pdf



[Instructions for use](#)

As-cast Austenite Grain Structure in Al Added 0.2 wt% Carbon Steel

Surya KENCANA,¹⁾ Munekazu OHNO,²⁾ Kiyotaka MATSUURA²⁾ and Kohichi ISOBE³⁾

1) Graduate Student, Graduate School of Engineering, Hokkaido University, North 13 West 8, Sapporo 060-8628 Japan.

2) Division of Materials Science and Engineering, Graduate School of Engineering, Hokkaido University, North 13 West 8, Sapporo 060-8628 Japan.

3) Muroran R&D Laboratory, Nippon Steel Corporation, 12, Nakamachi, Muroran 050-8550 Japan.

(Received on July 24, 2009; accepted on October 21, 2009)

Effects of Al addition on as-cast γ -austenite grain structure in 0.2wt%C–0.035wt%P steel with Al concentration ranging from 0.04 to 1.04 wt% were studied by means of furnace cooling and casting experiments. In the furnace cooling experiment with a cooling rate of 0.03°C/s, the as-cast γ grain structure consisted of equiaxed grains and the γ grain size was not affected by the increase in Al concentration up to 0.54 wt%. In the casting experiment of the sample with 0.04 wt% Al, on the other hand, the as-cast γ grain structure consisted of Coarse Columnar Grain (CCG), Fine Columnar Grain (FCG) and Equiaxed Grain (EG) regions, sequentially, from the mold side to the center of the ingot. The increase in Al concentration leads to increase in the fraction of FCG region at the expense of both CCG and EG regions. Even in the samples with high Al concentrations, AlN particles were rarely found and also Al segregation did not occur substantially. Instead, P segregated in interdendritic regions. The concentration of the segregated P increased from the CCG region to the FCG region. It was suggested based on a thermodynamic calculation that the segregation of P is enhanced by Al addition and the high P concentration stabilizes the high temperature phase such as liquid or δ -ferrite, depending on Al concentration at lower temperatures. This stabilized high temperature phase is considered to retard the γ grain boundary migration. Therefore, the increase of FCG region and the decreases of CCG and EG regions due to Al addition should be attributable to pinning effect of the stabilized high temperature phase.

KEY WORDS: carbon steel; solidification; δ - γ transformation; grain refinement; aluminum; phosphorous; segregation; pinning effect.

1. Introduction

Occurrence of transverse surface cracks in bending or straightening process of continually cast slabs of carbon steel and in subsequent rolling process is one of main obstacles in increasing the productivity in the Continuous Casting (CC) process. Studies on hot ductility in carbon steels reported that a decrement of hot ductility around the γ -austenite + α -ferrite two phase temperature region contributes to the occurrence of transverse surface cracks, and the decrement of hot ductility is essentially attributed to formation of coarse γ grain structure and the precipitation of fine particles along the γ grain boundary.^{1,2)} It was reported that hot ductility is inversely proportional to γ grain size.³⁾ Moreover, intergranular fracture is susceptible to the γ grain size and the transverse surface cracks were found to originate from the intergranular fracture of coarse γ grain.⁴⁾ Therefore, refinement of γ grains is one of the most important subjects to alleviate this problem.

Studies on evolution of γ grain structure during solidification and subsequent cooling process demonstrated that fine γ grains initially exist in presence of a secondary phase, *viz.*, δ -ferrite (or liquid) in the δ + γ (or γ +liquid)

two phase temperature region.^{3,5–7)} The fine γ grains then rapidly coarsen after disappearance of the secondary phase, *i.e.*, below T_γ , a temperature for completion of δ - γ transformation or γ -solidification. Therefore, the refinement of γ grains by lowering T_γ or stabilizing fine pinning particles has been attempted. The addition of ferrite stabilizing elements such as Nb, V, Mo or P was reported to refine the as-cast γ grains by lowering the T_γ .^{7,8)} Furthermore, the addition of carbide, nitride and carbonitride forming element such as Ti was reported to refine the as-cast γ grains by inhibiting γ grain growth with titanium carbonitride particles.^{9,10)}

Al is an important element to be added to low alloy steels for deoxidation process. On one hand, Al is well known as ferrite stabilizing element⁸⁾ and also, the Al addition to steel with a certain amount of N was reported to be effective in inhibiting γ grain growth by pinning effect of AlN during reheating prior to hot rolling process.^{11–13)} Nevertheless, the effects of Al addition on the as-cast γ grain structure have not been clarified in detail. The purpose of this study is to clarify the effects of Al addition on the as-cast γ grain structure. Focusing on 0.2 wt% C steel, we investigate the effects of Al concentration and cooling condition on the

as-cast γ grain structure, the variation of the as-cast γ grain size and morphology, and the correlation between the as-cast γ grain and δ dendrite structures.

2. Experimental Procedures

The carbon steel used in the present study is a hyperperitectic carbon steel with 0.2 wt% C. The chemical composition of the base steel is shown in **Table 1**. The effects of Al addition on the as-cast γ -austenite grain structure were investigated with different cooling experiments, furnace cooling and permanent mold casting experiments. The procedures of each experiment are explained as follows.

The Al concentration in the steel for the furnace cooling experiment was varied from 0.04 to 0.54 wt%. For the discussion described later, it should be noted that P concentration was 0.035 wt% in all the samples. The sample of 130 g was put in a cone shape alumina crucible and it was melted at 1550°C in a SiC electric furnace under Ar atmosphere. After holding for 1 h, the melt was cooled at cooling rate of 0.03°C/s. When the temperature reached 1100°C, the sample was quenched into a strongly stirred iced water bath. The quenched sample was then sectioned vertically in the middle part for microstructural examinations. The as-cast γ grain and δ dendrite structures were revealed using nital (3 vol%) and Oberhoffer's solutions, respectively. Based on the optical microscope observation, average γ grain size, d_γ , was evaluated by the equivalent area diameter method and secondary Dendrite Arm Spacing (DAS), λ_2 , was evaluated by the linear intercept method. A Scanning Electron Microscope (SEM) and an Electron Probe Micro Analyzer (EPMA) were employed for identification of fine particles.

In the permanent mold casting experiment, the Al concentration in the steel was varied from 0.04 to 1.04 wt%. The sample of 250 g was put in a magnesia crucible of a cylindrical shape with an inner diameter of 30 mm and a depth of 90 mm. The sample was melted at 1550°C in the SiC electric furnace under Ar atmosphere. After holding for 1 h, the melt was cast into a steel mold, which was held at room temperature before casting. The mold has a rectangular prism shape cavity and the detail of this mold shape can be found in Ref. 9). The cast sample shape was a rectangular

prism with a height of 40 mm, a width of 40 mm and a thickness of 20 mm.

Our preliminary casting experiments showed that when the sample was cooled down to room temperature, a large amount of α -ferrite phase precipitated on the γ grain boundary and also inside the γ grains and, accordingly, the prior γ grain structure was not clearly observed in the optical micrograph. Therefore, the following experiment was conducted to clearly observe the as-cast γ grain structure. The temperature of the ingot during the casting process was measured. The type-B thermocouple was inserted into the center of the mold cavity from the open upper side of the mold. The tip of the thermocouple was positioned at the center of the ingot and it was thinly coated with alumina cement to prevent a reaction with the molten steel. Based on the measured cooling curve, the casting sample was quenched from a temperature slightly above A_{r1} transformation temperature into the strongly stirred iced water bath. This procedure resulted in the microstructure consisting of film-like proeutectoid α -ferrite decorating the prior γ grain boundary and the martensite inside the prior γ grain, which enables a clear observation of the as-cast γ grain structure.

The quenched sample thus obtained was sectioned transversely at the middle of height. A rectangular area in the sectioned surface, extended from the mold side to the center in the thickness direction, was selected for microstructural examination with optical microscope. Similar to the furnace cooling experiment, the as-cast γ grain and δ dendrite structures were observed and identification of fine particles was performed.

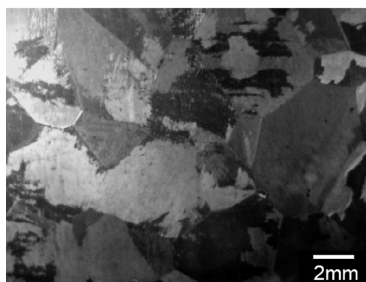
3. Results and Discussion

3.1. Furnace Cooling Experiment

Figures 1(a) and **1(b)** show the as-cast γ grain structures in the samples with Al concentrations of 0.04 and 0.54 wt%, respectively, after the furnace cooling experiment. In each sample, the as-cast γ grains are equiaxed ones and, importantly, the Al addition does not affect the γ grain size and morphology of γ grain structure. The relationship between the γ grain size, d_γ , and Al concentration is shown in **Fig. 2**. The γ grain size is about 4 mm regardless of Al concentration, indicating that the Al addition doesn't yield a significant change in the as-cast γ grain size. Furthermore, the relationship between secondary DAS, λ_2 , and Al concentration is also shown in **Fig. 2**. The secondary DAS takes approximately 0.7 mm regardless of Al concentration.

Table 1. The chemical composition of the base steel used in the present study in wt%.

C	Si	Mn	P	S	Al	N	O
0.199	0.20	0.80	0.035	0.007	0.040	0.006	0.002



(a)



(b)

Fig. 1. The as-cast γ grain structures of samples obtained from the furnace cooling experiment with a cooling rate of 0.03°C/s. (a) The sample with 0.04 wt% Al, (b) the sample with 0.54 wt% Al.

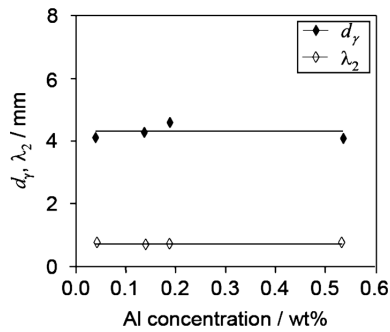


Fig. 2. The effects of Al concentration on as-cast γ grain size, d_γ , and secondary DAS, λ_2 , in samples obtained from the furnace cooling experiment with a cooling rate of 0.03°C/s , indicating the Al addition does not lead to substantial changes in d_γ and λ_2 .

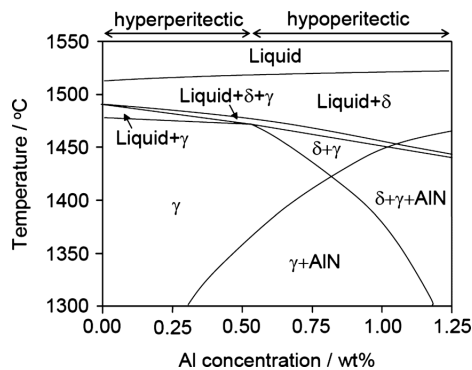


Fig. 3. A phase diagram of Fe-0.2wt%C-0.035wt%P-0.8wt%Mn-0.2wt%Si-0.006wt%N-xAl system obtained from CALPHAD method.

Figure 3 shows a phase diagram of Fe-0.2wt%C-0.035wt%P-0.8wt%Mn-0.2wt%Si-0.006wt%N-xAl system calculated from CALPHAD method.¹⁴⁾ We employed the thermodynamic database, PanIron for all the calculations.¹⁵⁾ The horizontal axis is Al concentration. The liquidus temperature does not substantially change with the Al concentration. It should be noticed that the type of steel changes from hyperperitectic to hypoperitectic one at 0.53 wt% Al. When Al concentration is less than 0.53 wt%, the solidus temperature, in other words, T_γ decreases very slightly with Al concentration. On the other hand, in the range of Al concentration for hypoperitectic steel, δ phase is stabilized at lower temperatures by increasing Al concentration, leading to drastic decrease in T_γ . As mentioned in the introduction, it has been reported that γ grains grow rapidly below T_γ and, therefore, lowering T_γ leads to finer γ grain structure. However, the decrement of T_γ up to 0.54 wt% Al is quite small. Therefore, the Al addition does not lead to significant change in the γ grain structure during slow cooling process, as is consistent with the result of Figs. 1 and 2. In Fig. 3, also, the temperature for formation of AlN phase increases with the increase in Al concentration. However, the AlN phase forms at much lower temperatures than T_γ in all samples of the present experiments. Hence, it is considered that the AlN phase precipitates from γ phase after γ grain growth substantially occurs at the high temperature region. In the present SEM/EPMA analysis, AlN particles were rarely detected.

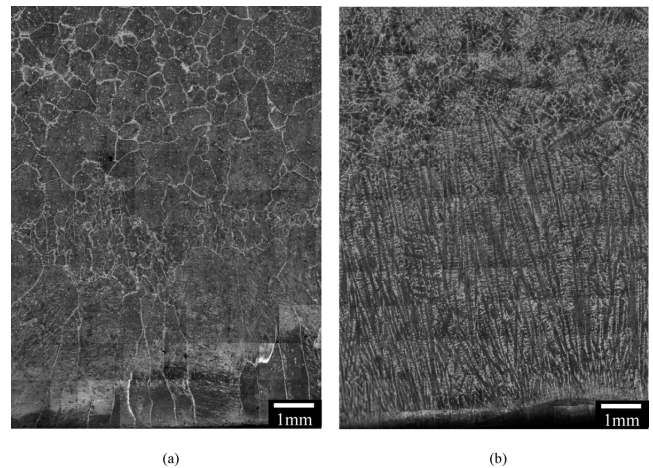


Fig. 4. Microstructures of the sample with 0.04 wt% Al obtained from the permanent mold casting experiment. (a) As-cast γ grain structure, (b) δ dendrite structure. The two photographs were taken at the same location in the sample. The top and the bottom of each micrograph correspond to the center of the ingot and the sidewall surface, respectively.

3.2. Casting Experiment

Figure 4(a) shows the as-cast γ grain structure in the sample with 0.04 wt% Al. As described in the Sec. 2, the γ grain boundary is decorated with film-like proeutectoid α phase. The bottom of the micrograph corresponds to the mold side, while the top part represents the center of the ingot. It is seen that the columnar grains develop from the mold side to the center of the ingot along the thickness direction, which coincides with the direction of heat flow in the present casting condition, and the equiaxed grains form in the central region. It is noted that very fine columnar grains form between the columnar grain region and the equiaxed grain region. Therefore, this as-cast γ grain structure can be characterized by three regions, Coarse Columnar Grain (CCG) region near the mold side, Equiaxed Grain (EG) region in the central region of the ingot, and Fine Columnar Grain (FCG) region in between the CCG and the EG regions.

Figure 4(b) shows the δ dendrite structure at the same location. The δ dendrite structure consists of columnar dendrites developing from the mold side to the inward of the sample and the equiaxed dendrites in the central region. By comparing the as-cast γ grain and δ dendrite structures (Figs. 4(a) and 4(b)), the CCG and FCG are found to originate from the columnar dendrites. The cooling rates at various positions from the mold side toward the center can be evaluated by the empirical equation, $\lambda_2 = 710(60\dot{T})^{-0.39}$, where the secondary DAS, λ_2 , is in mm and cooling rate, \dot{T} , is in $^\circ\text{C/s}$.¹⁶⁾ For example, the secondary DAS in the sample without Al addition were measured to be 45, 62 and 88 μm at 2, 4 and 8 mm from the mold side, respectively. Accordingly, the cooling rates are calculated to be 20, 9 and 4°C/s . These cooling rates are within the range of cooling rate of surface layer of continuously cast slab in carbon steel.¹⁷⁾

Figure 5(a) shows the as-cast γ grain structure in the sample with 0.54 wt% Al. As is similar to the structure in Fig. 4(a), the as-cast γ grain structure consists of the three regions, CCG, FCG and EG regions. Compared with the structure in Fig. 4(a), the area of CCG region is reduced,

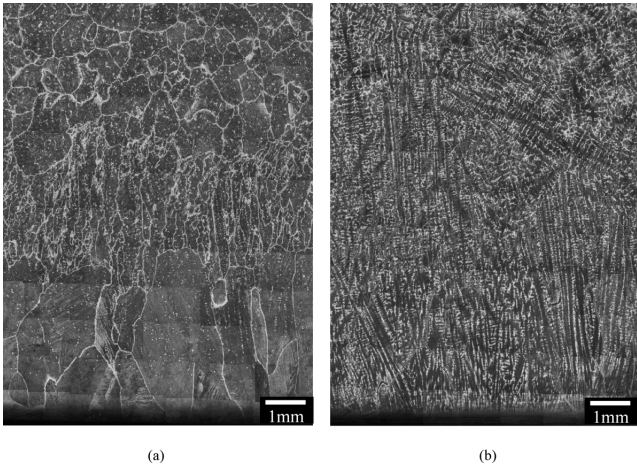


Fig. 5. Microstructures in the sample with 0.54 wt% Al obtained from the permanent mold casting experiment. (a) As-cast γ grain structure, (b) δ dendrite structure. The two photographs were taken at the same location in the sample. The top and the bottom of each micrograph correspond to the center of the ingot and the sidewall surface, respectively.

while the FCG region is extended. Figure 5(b) shows the δ dendrite structure at the same location. The δ dendrite structure consists of the columnar and equiaxed dendrites and it is not substantially different from the one with 0.04 wt% Al in Fig. 4(b).

The dependence of fractions of CCG, FCG and EG regions on Al concentration was investigated. The lengths of each region along the thickness direction were measured and these lengths were divided by the thickness of the observation area, *viz.*, 10 mm, to define the fraction of each region, f_i with $i = \text{CCG, FCG or EG}$. The results are shown in Fig. 6. As the Al concentration increases, the fractions of CCG and EG regions gradually decrease, while that of FCG region gradually increases. Hence, it can be said that the Al addition leads to the refinement of the as-cast γ grain structure in the permanent mold casting. In Fig. 6, furthermore, the fraction of columnar dendrite region, f_{CD} , is plotted. Although the data are scattered, f_{CD} seems to be independent of Al addition.

Next, the relationship between the γ grain size and Al concentration was investigated. The short axis diameters of CCG, $d_{\gamma\text{SCCG}}$, and FCG, $d_{\gamma\text{SFCG}}$, and the average diameter of EG, $d_{\gamma\text{EG}}$, are shown in Fig. 7. It is to be noted that the short axis diameters of CCG and FCG are almost independent of the Al concentration. However, the diameter of the EG gradually decreases with the increase in the Al concentration. The mechanism for this was considered similar to the increase of the FCG region, and will be discussed later. In Fig. 7, the primary DAS of columnar dendrite, λ_1 , at 4 mm from the mold side where the FCG always existed in all the samples and the center-to-center spacing of equiaxed dendrite, λ_c , are shown. The Al addition does not affect both the primary DAS and the center-to-center spacing of the equiaxed dendrite. It is important to note that the short axis diameter of FCG region is comparable to the primary DAS. This fact indicates that the grain growth of FCG in the short axis direction should have been inhibited immediately after the finish of the γ transformation.

It is expected from the phase diagram shown in Fig. 3

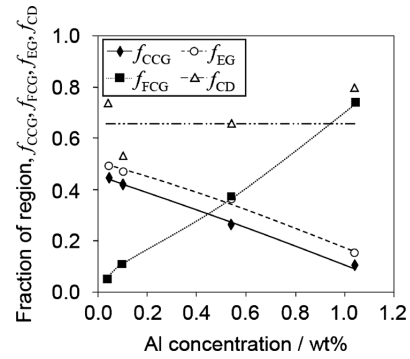


Fig. 6. The effects of Al concentration on the fractions of CCG, FCG and EG regions (f_{CCG} , f_{FCG} and f_{EG}) and the fraction of columnar dendrite region (f_{CD}).

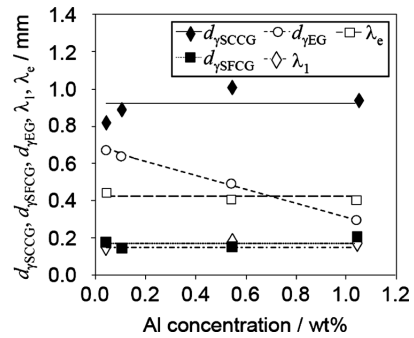


Fig. 7. The effects of Al concentration on the γ grain sizes. $d_{\gamma\text{SCCG}}$ and $d_{\gamma\text{SFCG}}$ represent the short axis diameters of CCG and FCG, respectively. $d_{\gamma\text{EG}}$ is the diameter of EG. λ_1 and λ_c are the primary DAS of columnar dendrites and the center-to-center spacing of equiaxed dendrites, respectively.

that Al addition produces the following two effects; the one is formation of AlN particles at higher temperatures and the other is stabilization of δ phase at lower temperatures. As discussed in Fig. 2, the Al addition did not affect the as-cast γ grain structure in the furnace cooling experiment of which condition should be close to the equilibrium solidification condition. However, as shown in Figs. 6 and 7, the Al addition results in the significant change in the as-cast γ grain structure in the casting experiment which may correspond to non-equilibrium solidification condition. It is very likely that significant segregation of Al occurs during the casting experiment because of the high cooling rate. In Fig. 3, it can be seen that the formation temperature of AlN increases with Al concentration, and therefore, the Al segregation produces an increase in the formation temperature of AlN in the segregation region. Then, it may be possible that AlN particles form in the region of Al segregation before the γ grain growth takes place and they act as pinning particles. In order to examine the existence of AlN particles, we performed SEM/EPMA analysis. In the samples without Al addition and with 0.1 wt% Al, AlN particle was not found. In the samples with 0.54 and 1.04 wt% Al, the AlN particles with a size of about 1 μm were observed and, however, there were only a few particles dispersed. Later, we discuss the possibility that the pinning effect is produced by finer AlN particles with size of less than 1 μm which precipitate from γ phase.

As already pointed out in Fig. 3, the steel with Al more than 0.53 wt% is of hypoperitectic type and the δ -ferrite

phase is stabilized at lower temperatures by the high Al concentration. The stabilization of δ phase leads to the decrease in T_γ and finally to the γ -grain refinement due to the pinning effect of the stabilized δ -ferrite. In order to examine the occurrence of Al segregation, the sample was quenched from 1000°C. The sample with 0.54 wt% Al was cast into the permanent mold and it was then quenched after 60 s from casting by dropping into the strongly stirred iced water bath. The 60 s was the length of time spent for the decrease in temperature from the casting temperature to 1000°C at the center of the ingot, according to the recorded cooling curve. This sample was subjected to EPMA analysis. The EPMA analysis was performed at every 1 μm along a 400 μm distance parallel to the mold wall in both CCG and FCG regions. The Al concentration profiles in CCG and FCG regions are shown as white plots in the upper part of Figs. 8 and 9, respectively, where Al concentration is indicated in wt% by the vertical axis on the left-hand side and the distance of EPMA analysis is indicated in mm by the horizontal axis. Although the data are scattered, the Al concentration profiles in both CCG and FCG regions appear to be almost constant at approximately 0.5 wt%. This indicates that Al segregation does not occur substantially. A detailed comparison between these profiles and δ dendrite structures indicates that Al concentration takes slightly high values at columnar dendrite stems, while Al

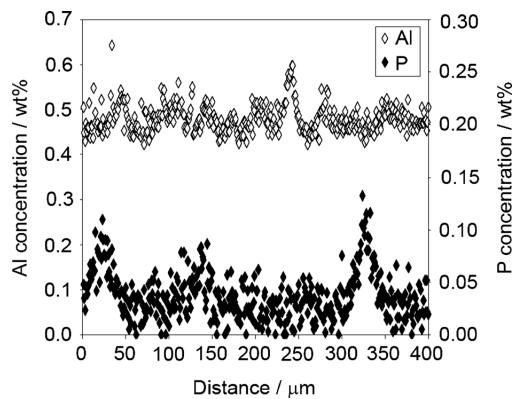


Fig. 8. Concentration profiles of Al and P in the CCG region of the cast sample with 0.54 wt% Al. The scanned direction is parallel to the mold wall. White and black plots represent Al and P concentration profiles, respectively.

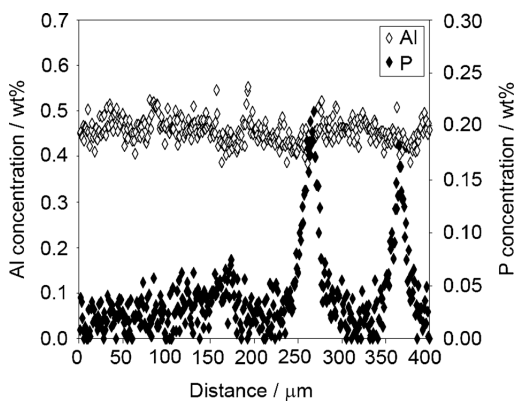


Fig. 9. Concentration profiles of Al and P in the FCG region of the cast sample with 0.54 wt% Al. The scanned direction is parallel to the mold wall. White and black plots represent Al and P concentration profiles, respectively.

depletion occurs at columnar interdendritic regions, which is consistent with the fact that the partition coefficient of Al for δ phase in this steel, k_{Al} , is calculated to be larger than 1, $k_{Al}=1.25$, from the CALPHAD method. It is important to note that since Al segregation does not occur significantly, the formation temperature of AlN phase is much lower than T_γ in the entire sample as is seen in Fig. 3. Therefore, if very fine AlN particles with size of less than 1 μm exist in the sample, such particles are those precipitated from the γ phase after γ grain growth. Therefore, such very fine particle should not be responsible for the change of as-cast γ grain structure as seen from Figs. 4(a) to 5(a).

Since Al segregation does not occur significantly in both CCG and FCG regions, the segregation of another solute element should be responsible for the changes in the γ grain structure. Among the elements contained in the present steel, P is known as a strong ferrite stabilizing element. In the present casting sample, the total amount of P is 0.035 wt%. The P concentration profiles in CCG and FCG regions are shown as black plots in Figs. 8 and 9, respectively, where P concentration is indicated by the vertical axis on the right-hand side. It can be seen that in both CCG and FCG regions, the P segregation clearly occurs. It was revealed from the comparison between these profiles and the δ dendrite structures that the positions where the P concentration takes high values correspond to interdendritic regions of columnar dendrites. Importantly, the concentrations of the segregated P in the FCG regions are significantly higher than those in the CCG region.

The segregations of the other elements should be addressed. The effect of segregations of N, O and S during solidification is considered negligible, because the concentrations of these elements are quite small in the present samples. Among the other elements, the partition coefficient of C during δ solidification process is lowest and its average concentration is 0.2 wt% and, hence, the behavior of C concentration is of critical importance to determine the solidification process. However, the diffusion coefficient of C is quite high even in the δ and γ phases and it is basically safe to assume that the C concentration takes almost equilibrium value under a given condition during the present casting experiment. Therefore, the effect of the segregation of C on the formation of γ grain structure should be negligible. In addition, our EPMA analysis demonstrated that the concentrations of Si and Mn are almost uniform over the samples. The Mn concentration slightly takes high value of about 1.2 wt% at interdendritic position of FCG region. However, our calculation for phase equilibria indicated that this slight change in the Mn concentration does not substantially alter the phase equilibria and the discussion described in the following. Therefore, the segregation of P is considered to play the most important role in the present refinement effect.

Suzuki *et al.*¹⁸⁾ reported that P addition to hyperperitectic steels with C higher than 0.25 wt% causes enrichment of P concentration in liquid film of the interdendritic region during the solidification process. Accordingly the liquid remains at low temperatures, *viz.*, the P addition lowers the T_γ of the hyperperitectic steels. Moreover, Yoshida *et al.*⁸⁾ reported that P addition to hypoperitectic steel of 0.1 wt% C

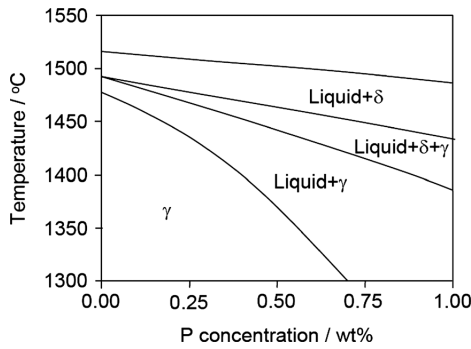


Fig. 10. A phase diagram of Fe-0.2wt%C-0.04wt%Al-0.8wt%Mn-0.2wt%Si-0.006wt%N-xP system obtained from CALPHAD method.

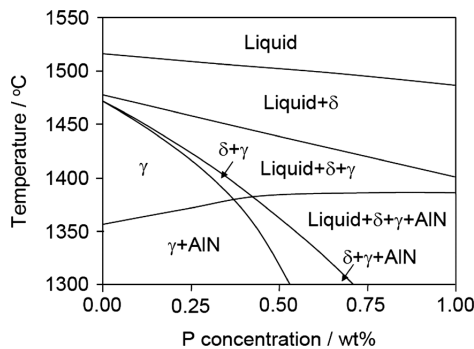


Fig. 11. A phase diagram of Fe-0.2wt%C-0.54wt%Al-0.8wt%Mn-0.2wt%Si-0.006wt%N-xP system obtained from CALPHAD method.

results in refinement of the as-cast γ grain structure. The P addition leads to stabilization of δ phase which effectively inhibits γ grain growth in the $\delta+\gamma$ region. Therefore, the P addition stabilizes the liquid for a hyperperitectic steel and the δ -ferrite for a hypoperitectic steel at lower temperatures. As shown in Fig. 3, the present samples with Al less than 0.53 wt% correspond to the hyperperitectic steel, while the ones with Al more than 0.53 wt% are the hypoperitectic steel. The phase diagrams of 0.2 wt% C steel with 0.04 wt% Al and 0.54 wt% Al are shown in **Figs. 10** and **11**, respectively. The horizontal axis is P concentration. As shown in these figures, the increase in P concentration causes a significant decrease in T_γ in both cases. Therefore, the P addition and/or segregation lead to the pinning effect on γ grain growth due to stabilization of the high temperature phases that play a role as the pin. The pinning phase corresponds to the liquid phase in the hyperperitectic steel and the δ phase in the hypoperitectic steel. It is noted that the partition coefficient of P for $\delta+L$ phase field is much less than 1 and the P always segregates in the interdendritic region as is observed in the present study. Therefore, the pinning phase may always exist at interdendritic region regardless of the type of pinning phase.

As described above, all the samples discussed so far contained 0.035 wt% P. In order to see the effect of P concentration on the γ grain structure, we performed the casting experiment of the sample with 0.04 wt% Al and 0.015 wt% P. The result is shown in **Fig. 12**. One can see that the structure consists of only the CCG and the EG and there is no FCG region. Therefore, it can be concluded that the formation FCG region shown in Fig. 4 originates from the effect



Fig. 12. As-cast γ grain structure in the sample with 0.015 wt% P obtained from the permanent mold casting experiment. The top and the bottom of the micrograph correspond to the center of the ingot and the sidewall surface, respectively.

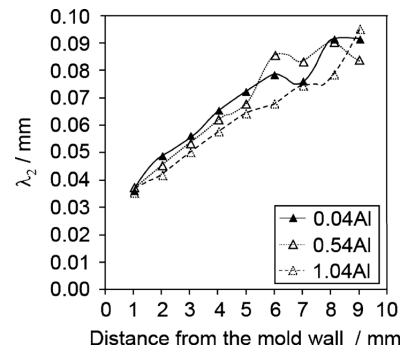


Fig. 13. The secondary DAS versus the distance from the mold wall in samples with different Al concentrations.

of P, more precisely, segregation of P.

In all samples of the present study, the FCG region was found in between the CCG and EG regions. The results of EPMA analysis shown in Figs. 8 and 9 demonstrate that the concentration of segregated P is higher in the FCG region than in the CCG region. **Figure 13** shows the secondary DAS versus the distance from the mold wall to center in samples with different Al concentrations. The dependence of secondary DAS on the distance is not significantly different in all the samples. Importantly, the secondary DAS increases from the mold side to the center of the ingot, which indicates that the cooling rate decreases from the mold side to the center. Therefore, the cooling rate in CCG region should be higher than that in the FCG region. A number of experiments for solidification under negligible temperature gradients¹⁹⁻²¹⁾ demonstrated that the degree of microsegregation decreases with the decrease in cooling rate and this fact can be commonly explained by Brody-Flemings (B-F) model,²²⁾ Clyne-Kurz (C-K) model²³⁾ and numerical simulations.^{24,25)} On the contrary, several studies for microsegregation in directionally solidified or mold casting samples^{21,26-29)} found an increase in microsegregation from the mold side to the center of ingot, which is consistent with our observation. Although the B-F and C-K models assume the uniform distribution of solute elements

in liquid phase, Doherty *et al.*,²¹⁾ Weinberg *et al.*²⁷⁾ and Sugiyama *et al.*³⁰⁾ suggested that during the initial solidification stage near the mold side, the diffusion layer exists ahead of solid–liquid interface and, hence, the effective partition coefficient increases with the cooling rate according to Bolling–Tiller model.³¹⁾ Their suggestion results in the less microsegregation in the mold side compared with the center part of the ingot. In addition, other explanations were proposed for the increase in the microsegregation from the mold side to the center.^{26,28)} Also, the morphology of the dendrite structure should be closely related to the degree of microsegregation. **Figure 14** shows the dependency of the primary DAS on the distance from the mold wall toward center of ingot in the samples with different Al concentrations. The primary DAS increases from the mold side toward the center and this behavior is almost identical in all the samples. The increment of the primary DAS indicates the decrease in the number of the columnar dendrites due to competitive growth process between the neighboring columnar dendrites. Accordingly, the interdendritic regions between the columnar dendrites, *viz.*, the possible segregation sites decrease from the mold side to the center, which may lead to the increase in degree of the microsegregation per the site from the mold side to the center. Therefore, we consider that in our sample one or some of the proposed mechanisms took place to produce higher microsegregation of P in FCC region, although we cannot provide the conclusive evidence regarding which mechanism should be dominant. Based on the microsegregation of P, the formation process of FCG region in hyperperitectic steel can be explained as follows. **Figure 15** represents the schematic illustrations of the formation process of FCG region in hyperperitectic steel. During solidification process, the stabilized high temperature phase, liquid (or δ -ferrite in hypoperitectic steel), does not appear in CCG region (Fig. 15(a)) since the segregation of P is not substantial and the γ grain growth significantly occurs in this region without the pinning effect due to the coexisting second phase. Such γ grains develop with columnar shape along the temperature gradient in the thickness direction of the ingot. The development of these coarse columnar grains is stopped at a position where the stabilized high temperature phase exists due to the high concentration of P segregated in the interdendritic region. The coexisting phase prevents the further growth of the CCG and promotes the formation of new γ -grains. The newly formed γ grains develop with the columnar shape due to the temperature gradient (Fig. 15(b)). These new columnar grains cannot grow in the short axis direction since the pinning phase exists in the interdendritic region, hence, the short axis diameter of these columnar grains should become comparable to the primary dendrite arm spacing and these grains correspond to the FCG (Fig. 15(c)). In the central part of the ingot, the equiaxed γ grains form from the equiaxed dendrite. Even though there is a large degree of microsegregation of P in this region just after solidification, the microsegregation of P should be reduced during the cooling process with a low cooling rate (Fig. 15(d)). Hence the γ grain can grow to form EG region. Finally, the as-cast γ grain structure consists of CCG, FCG and EG regions (Fig. 15(e)). The formation process of the as-cast γ grain structure in hypoperitectic steel is almost similar to that given in Fig. 15, except

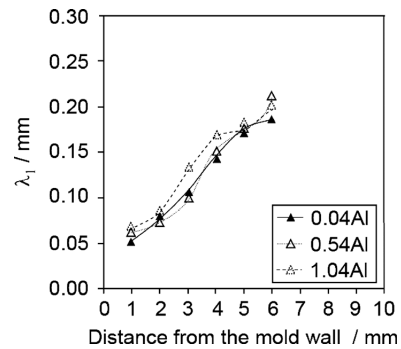


Fig. 14. The primary DAS versus the distance from the mold wall in samples with different Al concentrations.

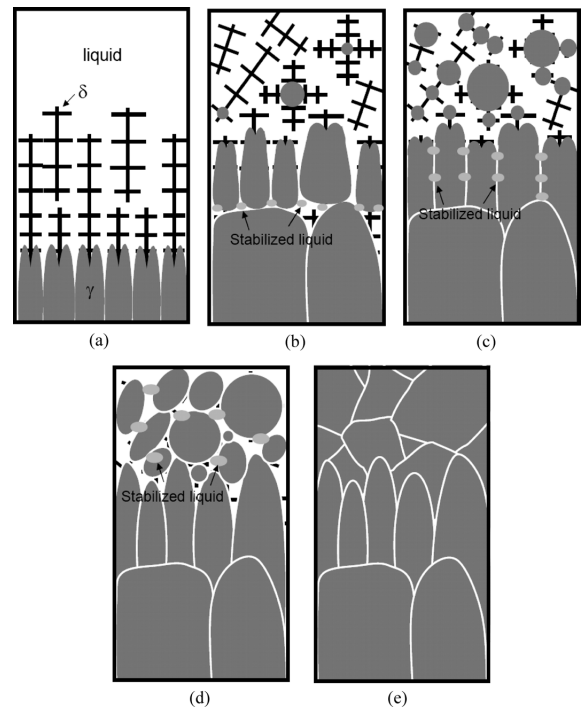


Fig. 15. Schematic illustrations of formation process of CCG, FCG and EG regions in hyperperitectic steel. The top and bottom of each illustration correspond to the center of ingot and the sidewall surface, respectively. (a) At the beginning of solidification, columnar dendrites grow toward the center of the ingot followed by the γ transformation. (b) Coarse columnar γ grains are developed while the high temperature phase (liquid) is stabilized at lower temperatures due to P segregation, which inhibits further development of coarse γ grains. Then, columnar γ grains newly form ahead of the coarse columnar grains. (c) The coarsening of these newly formed columnar grains along short axis direction is prohibited by the pinning effect of the high temperature phase. The equiaxed γ grain forms in the center area where the temperature gradient is smaller and the cooling rate is lower. (d) The high temperature phase may be also stabilized in the equiaxed region. However, due to the slow cooling rate, the P segregation is reduced and the high temperature phase disappears. (e) Finally, the γ grain structure consists of CCG, FCG and EG regions.

that the stabilized pinning phase is δ phase.

As discussed above, the formation of FCG should be ascribable to the pinning effect of the high temperature phase (liquid or δ phase) stabilized by the P segregation. On the other hand, it was observed in Fig. 6 that despite that the

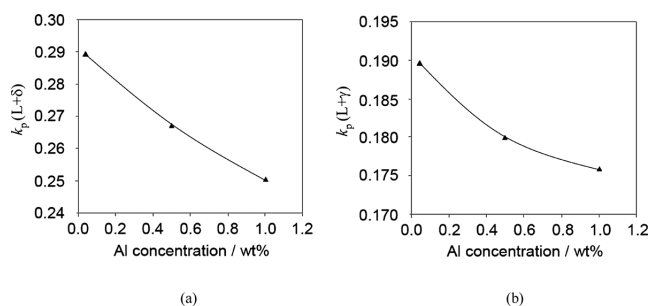


Fig. 16. The dependency of the equilibrium partition coefficient of P, k_p , on Al concentration in Fe-0.2wt%C-0.035wt%P-0.8wt%Mn-0.2wt%Si-0.006wt%N-xAl system calculated from CALPHAD method. (a) The partition coefficient of P during δ phase solidification at liquidus temperature, (b) The partition coefficient of P during γ phase solidification at solidus temperature.

total P concentration was fixed, the fraction of FCG region increases with the increase in Al concentration. **Figure 16(a)** shows the relationships between the equilibrium partition coefficient of P for δ +L phase equilibrium, k_p , and Al concentration at liquidus temperature. Also, **Fig. 16(b)** demonstrates the partition coefficient of P between γ and L phases at solidus temperature. These relationships were obtained using CALPHAD method for an alloy system of Fe-0.2wt%C-0.035wt%P-0.8wt%Mn-0.2wt%Si-0.006wt%N-xAl. The Al addition reduces the partition coefficients of P, which indicates that Al addition promotes the P segregation. Therefore, the Al addition results in stabilization of pinning phase due to the P segregation, which is considered to increase the fraction of FCG region (**Fig. 6**) and also slight decrement of EG diameter (**Fig. 7**). The present results demonstrate that the grain refinement effect due to P segregation can be enhanced by the Al addition.

4. Conclusions

Effects of Al addition on as-cast γ grain structure of 0.2 wt% C steel were studied in furnace cooling and permanent mold casting experiments. The important findings are summarized as follows.

(1) In the furnace cooling experiment with a cooling rate of 0.03°C/s, the as-cast γ grain structure consisted of equiaxed grains. The Al addition with a range of 0.04–0.54 wt% did not affect both the γ grain size and secondary dendrite arm spacing of the δ dendrite structure.

(2) In the casting experiment, the as-cast γ grain structure consisted of Coarse Columnar Grain (CCG) region near the mold wall, Fine Columnar Grain (FCG) region next to the CCG region and Equiaxed Grain (EG) region in the center of the mold thickness. The Al addition increased the FCG region at the expense of both the CCG and EG regions, and furthermore it reduced the diameter of the EG. The as-cast δ dendrite structure consisted of columnar dendrite and equiaxed dendrite regions. The fractions of these regions, and primary and secondary dendrite arm spacing did not change with the addition of Al.

(3) The short axis diameter of FCG was comparable to the primary dendrite arm spacing of columnar dendrite,

which indicates the γ grain growth along the short axis direction is inhibited immediately after the finish of the γ transformation.

(4) According to the SEM/EPMA analysis, only a few AlN particles with size of $\sim 1 \mu\text{m}$ were observed in the casting samples. The EPMA analysis demonstrated that Al segregation does not occur significantly, while P segregates in the interdendritic regions. The concentration of the segregated P increased from the CCG region to the FCG region.

(5) The thermodynamic calculation indicated that the high P concentration stabilizes the high temperature phase, liquid phase for the sample with less than 0.53 wt% Al and δ phase for the sample with more than 0.54 wt% Al, at lower temperatures. These high temperature phases are considered to inhibit the γ grain growth. Importantly, the segregation of P is enhanced by the addition of Al.

REFERENCES

- H. G. Suzuki, S. Nishimura and S. Yamaguchi: *Trans. Iron Steel Inst. Jpn.*, **22** (1982), 48.
- C. Ouchi, K. Matsumoto: *Trans. Iron Steel Inst. Jpn.*, **22** (1982), 181.
- Y. Maehara, K. Yasumoto, Y. Sugitani and K. Gunji: *Trans. Iron Steel Inst. Jpn.*, **25** (1985), 1045.
- L. Schmidt and A. Josefsson: *Scand. J. Metall.*, **3** (1974), 193.
- N. S. Pottore, C. I. Garcia and A. J. DeArdo: *Metall. Trans. A*, **22A** (1991), 1871.
- T. Maruyama, K. Matsuura, M. Kudoh and Y. Itoh: *Tetsu-to-Hagané*, **85** (1999), 585.
- T. Maruyama, M. Kudoh and Y. Itoh: *Tetsu-to-Hagané*, **86** (2000), 14.
- N. Yoshida, O. Umezawa and K. Nagai: *ISIJ Int.*, **43** (2003), 348.
- M. Ohno and K. Matsuura: *ISIJ Int.*, **48** (2008), 1373.
- M. Sasaki, K. Matsuura, K. Ohsasa, M. Ohno: *Tetsu-to-Hagané*, **94** (2008), 31.
- D. Hall and G. H. J. Bennett: *J. Iron Steel Inst.*, **205** (1967), 309.
- L. J. Cuddy and J. C. Raley: *Metall. Trans. A*, **14A** (1983), 1989.
- N. Gao and T. N. Baker: *ISIJ Int.*, **38** (1998), 744.
- L. Kaufman and H. Bernstein: *Computer Calculation of Phase Diagrams with Special Reference to Refractory Materials*, Academic Press, New York, (1970), 1.
- <http://www.computherm.com/databases.html>.
- A. Suzuki, T. Suzuki, Y. Nagaoka and Y. Iwata: *J. Jpn. Inst. Met.*, **32** (1968), 1301.
- N. Yoshida, Y. Kobayashi and K. Nagai: *Tetsu-to-Hagané*, **90** (2004), 16.
- H. G. Suzuki, S. Nishimura and Y. Nakamura: *Trans. Iron Steel Inst. Jpn.*, **24** (1984), 54.
- A. B. Michael and M. B. Bever: *Trans. AIME*, **200** (1954), 47.
- O. Hammar and G. Grömbaum: *Scand. J. Metall.*, **3** (1974), 11.
- R. D. Doherty and D. A. Melford: *J. Iron Steel Inst.*, **204** (1966), 1131.
- H. D. Brody and M. C. Flemings: *Trans. TMS-AIME*, **236** (1966), 615.
- T. W. Clyne and W. Kurz: *Metall. Trans. A*, **12A** (1981), 965.
- T. Matsumiya, H. Kajioaka, S. Mizoguchi, Y. Ueshima and H. Esaka: *Trans. Iron Steel Inst. Jpn.*, **24** (1984), 873.
- Y. Ueshima, S. Mizoguchi, T. Matsumiya and H. Kajioaka: *Metall. Trans. B*, **17B** (1986), 845.
- T. Z. Kattamis and M. C. Flemings: *Trans. AIME*, **223** (1965), 992.
- F. Weinberg and E. Teghtsoonian: *Metall. Trans.*, **3** (1972), 93.
- D. A. Granger and T. F. Bower: *J. Inst. Met.*, **98** (1970), 353.
- P. J. Ahearn and C. Quigley: *J. Iron Steel Inst.*, **204** (1966), 16.
- M. Sugiyama, T. Umeda and J. Matsuyama: *Tetsu-to-Hagané*, **60** (1974), 1094.
- G. F. Bolling and W. A. Tiller: *J. Appl. Phys.*, **32** (1961), 2587.